

Influence of ion species on extraction characteristics of mixed ion beams

Ao Xu(徐翱), Pingping Gan(甘娉娉), Xiang Wan(万翔), and Yuanjie Shi(石元杰)

Citation: Chin. Phys. B, 2024, 33 (**9**): 095202. DOI: 10.1088/1674-1056/ad5c3d
Journal homepage: http://cpb.iphy.ac.cn; http://iopscience.iop.org/cpb

What follows is a list of articles you may be interested in

Influence of extraction voltage on electron and ion behavior characteristics

Ao Xu(徐翱), Pingping Gan(甘娉娉), Yuanjie Shi(石元杰), and Lei Chen(陈磊)
Chin. Phys. B, 2024, 33 (**4**): 045203. DOI: 10.1088/1674-1056/ad1820

Theoretical analyses on the one-dimensional charged particle transport in a decaying plasma under an electrostatic field

Yao-Ting Wang(汪耀庭), Xin-Li Sun(孙鑫礼), Lan-Yue Luo(罗岚月), Zi-Ming Zhang(张子明), He-Ping Li(李和平), Dong-Jun Jiang(姜东君), and Ming-Sheng Zhou(周明胜)
Chin. Phys. B, 2023, 32 (**9**): 095201. DOI: 10.1088/1674-1056/ace033

Disruption prediction based on fusion feature extractor on J-TEXT

Wei Zheng(郑玮), Fengming Xue(薛凤鸣), Zhongyong Chen(陈忠勇), Chengshuo Shen(沈呈硕), Xinkun Ai(艾鑫坤), Yu Zhong(钟昱), Nengchao Wang(王能超), Ming Zhang(张明),Yonghua Ding(丁永华), Zhipeng Chen(陈志鹏), Zhoujun Yang(杨州军), and Yuan Pan(潘垣)
Chin. Phys. B, 2023, 32 (**7**): 075203. DOI: 10.1088/1674-1056/acc7fc

Hybrid-PIC/PIC simulations on ion extraction by electric field in laser-induced plasma

Xiao-Yong Lu(卢肖勇), Cheng Yuan(袁程), Xiao-Zhang Zhang(张小章), Zhi-Zhong Zhang(张志忠)
Chin. Phys. B, 2020, 29 (**4**): 045201. DOI: 10.1088/1674-1056/ab75d8

A miniaturized 2.45 GHz ECR ion source at Peking University

Jia-Mei Wen(温佳美), Shi-Xiang Peng(彭士香), Hai-Tao Ren(任海涛), Tao Zhang(张滔), Jing-Feng Zhang(张景丰), Wen-Bin Wu(武文斌), Jiang Sun(孙江), Zhi-Yu Guo(郭之虞), Jia-Er Chen(陈佳洱)
Chin. Phys. B, 2018, 27 (**5**): 055204. DOI: 10.1088/1674-1056/27/5/055204

Influence of ion species on extraction characteristics of mixed ion beams

Ao Xu(徐翱), Pingping Gan(甘娉娉)†, Xiang Wan(万翔), and Yuanjie Shi(石元杰)

Institute of Electronic Engineering, China Academy of Engineering Physics, Mianyang 621999, *China*

(Received 17 April 2024; revised manuscript received 24 June 2024; accepted manuscript online 27 June 2024)

The spatial distributions of different kinds of ions are usually not completely the same in the process of extracting. In order to study the reason for the different characteristics of ion extraction, a simplified simulation model of Cu^+ and Cr^+ ions extraction process was established by 2D3V (two-dimensional in space and three-dimensional in velocity space) particle-in-cell (PIC) method. The effects of different extraction voltages from 0 V to 500 V on the density distribution of Cu^+ and Cr^+ ions and the change of plasma emission surface were analyzed. On the basis of this model, the ion density distribution characteristics of Cu^+ ions mixed with Li^+, Mg^+, K^+, Fe^+, Y^+, Ag^+, Xe^+, Au^+, and Pb^+ ions respectively under 200-V extraction voltage are further simulated, and it is revealed that the atomic mass of the ions is the key reason for different ion density distributions when different kinds of ions are mixed and extracted, which provides support for further understanding of ion extraction characteristics.

Keywords: extraction, ion species, density distribution, atomic mass

PACS: 52.65.–y, 52.65.Rr, 29.25.–t, 29.25.Ni **DOI:** 10.1088/1674-1056/ad5c3d

1. Introduction

Ions produced by the ion sources can be extracted and transported under the action of electric field, and have wide applications.[1–3] Therefore, many researchers are concerned about the characteristics of extracted ions.[4,5] Li presented a two-dimensional (2D) model to simulate the ion optics for ion extraction, and pointed out that the thermal velocities of ions could affect the perveance condition of the ion beams.[6] Abdelrahman investigated ion beam dynamics and compared the emittance to aberration ratios of two- and three-electrode extraction systems.[7] Xu simulated plasma motion and ion extraction characteristics under different conditions, and obtained that the space charge force formed by the relative aggregation of positive and negative net charges is the main reason for the variation of extraction current.[8] Shmelev simulated the plasma jet formation in vacuum arc by using a hybrid model, and found that the light ions could expand faster than the heavy ions.[9] Keller viewed the ion beam formation process and extraction system of high current beams extracted from ion sources, and derived a general scaling model of extraction systems for a wide range of beam current and energy values.[10] Chen employed a PIC code to simulate the parallel-plate ion extraction process under an externally applied electrostatic field, and showed that initial electron temperature could affect the ion extraction time and the ion flux to the positive plate.[11] In addition, the plasma-sheath,[12–15] and the space charge limited current[16–18] related to ion extraction have also been widely concerned. However, these studies focus more on the main factors affecting the intensity and distribution of ion current, the design of ion extraction structure, the characteristics of ion emission surface, and so on. There are few studies on the interaction between different kinds of ions during the extraction of mixed ions.

In this paper, the density distribution of electrons, Cu^+ ions, and Cr^+ ions in the extraction process and the influence of extraction voltage on the distribution of these particles and the plasma emission surface are analyzed by establishing a simplified 2D simulation model of low-voltage extraction of Cu^+ ions mixed with Cr^+ ions. Furthermore, the density distribution of different particles when Cu^+ ions are mixed with other kinds of ions is simulated, and the main reasons affecting the ion density distribution are analyzed, which provides theoretical support for further deepening the ion extraction characteristics.

2. Simulation model

Based on 2D3V (two-dimensional in space and three-dimensional in velocity space) PIC method,[19] a simulation model of plasma diffusion and extraction is established. The PIC code we used has been compared and verified with experimental results of related plasma characteristics for many times,[20,21] and is often used in the simulation study of plasma characteristics.[22–24] The schematic diagram is shown in Fig. 1. The model consists of a plasma chamber, grids, and an extraction electrode. They are made of metal. The calculated area is 5 mm×5 mm. The wall thickness, inner length, and width of the plasma chamber are 0.1 mm, 4.8 mm, and 2.5 mm, the grid length and width are 0.05 mm and 0.1 mm, the distance between the plasma chamber and the extraction electrode is 2.4 mm, and the plasma injection area is 1-mm long. The extraction electrode is connected with negative volt-

†Corresponding author. E-mail: pingping.0224@qq.com

© 2024 Chinese Physical Society and IOP Publishing Ltd

age, the plasma chamber and grid are grounded, and the area without electrodes on both sides is set as Neumann boundary condition.

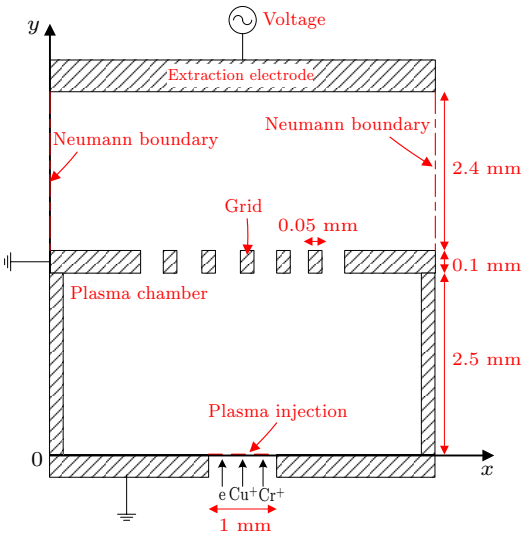


Fig. 1. Schematic diagram of simulation area.

The simulated particles are electrons, Cu^+, and Cr^+. As the density and temperature of the plasma are relatively low, the influence of the interaction between the particles and the wall on the plasma motion can be neglected. Therefore, the secondary electron effect produced by particle bombardment on the wall of the device is not considered. All the particles bombarded on the surface of the metallic device wall are absorbed, and the surface charge accumulation effect is not considered. In addition, the PIC method tracks the motion of electrons and ions, and calculates the Coulomb collisions among these charged particles, but ignores the elastic collisions and the possible chemical reactions. In the plasma injection area the flux of the electrons is set as 2×10^{21} $m^{-2}\cdot s^{-1}$ with temperature of 5.0 eV and velocity of 1×10^5 $m\cdot s^{-1}$, and the flux of Cu^+ is set as 1×10^{20} $m^{-2}\cdot s^{-1}$ with temperature of 0.1 eV and velocity of 1×10^4 $m\cdot s^{-1}$. In order to reach the plasma condition, the parameters of Cr^+ is set the same as those of Cu^+. In addition, the time step of the simulation is 10^{-12} s, and the space step is 0.025 mm.

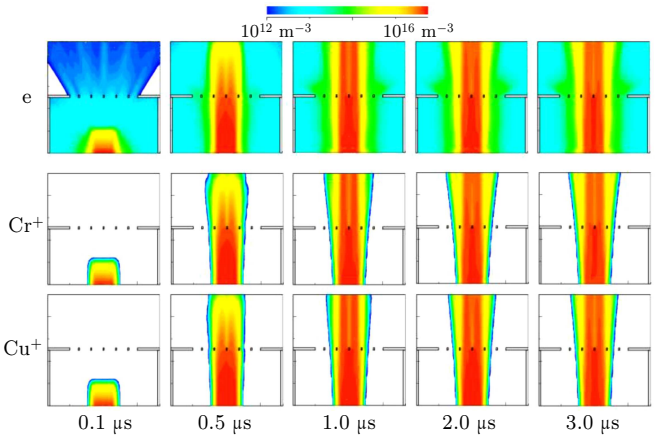


Fig. 2. Density distributions at different time.

Through many times of simulation calculations and comparisons, we obtained that the simulation results converges stably at 3 μs, as shown in Fig. 2. Therefore, the results at 3 μs are discussed in subsequent sections.

3. Simulation results

Based on the simulation model in the previous section, the extraction electrode is connected with 1×10^{-6} V (close to 0 V, because in the code the voltage cannot directly be set as 0 V), −50 V, −100 V, −200 V, −300 V, and −500 V. The density distribution of electrons, Cu^+, and Cr^+ under different extraction voltage conditions at 3 μs are obtained, as shown in Fig. 3. Due to the existence of the extraction voltage, the electron density distribution is obviously different from the positive ion density distribution, but the density distributions of Cr^+ ions and Cu^+ ions are relatively similar. With the increase of the amplitude of the extraction voltage, the suppression of electrons becomes stronger. When the amplitude of the extraction voltage increases to 300 V, most electrons are suppressed in the plasma chamber. This means that the position of separation between electrons and positive ions is closer to the plasma chamber with the increase of the amplitude of the extraction voltage. When the amplitude of the extraction voltage increases to 300 V, the separation between electrons and positive ions begins near the grids. This leads to the farthest distance between the separated positive ions and the extraction electrode, and the separated positive ions will diffuse continuously under the action of the space charge force, results in the largest divergence of ion beam. When the amplitude of the extraction voltage increases to 500 V, the extraction electric field begins to extend into the plasma chamber, which leads to the formation of a focusing electric field force between the grid and the extraction electrode, thus the ion beam is confined and the divergence angle of the ion beam decreases instead. However, the density distributions of Cr^+ ions, Cu^+ ions, and electrons are almost the same in the plasma chamber when the amplitude of the extraction voltage varies from 0 V to 500 V, which is due to the fact that the extraction electric field is almost shielded by the plasma chamber, so that there is no external electric field in the plasma chamber to affect the motion behaviors of electrons and positive ions, and positive ions and electrons are attracted to each other only by the space charge force formed by plasma, thus moving together.

The change of separation position between electrons and positive ions caused by different extraction voltage amplitudes also makes the potential distribution change, as shown in Fig. 4. It can be found that when the extraction voltage is basically 0 V, the potential of the whole simulation area is less than 1 V. When the negative extraction voltage appears, the positive ions separated from electrons diffuse outward due to their own space charge force and the external field, which

forms a convex surface with approximate zero potential distribution outside the plasma chamber and near the separation position between electrons and positive ions (that is, the position where plasma conditions are no longer met). This convex surface of approximate zero potential distribution is defined as the plasma emission surface. With the increase of the amplitude of the extraction voltage, the plasma emission surface is continuously compressed towards the grids. When the amplitude of the extraction voltage increases to more than 300 V, the plasma emission surface gradually changes from convex to plane. The potential distributions at the grids under different extraction voltages are shown in Fig. 5. The extraction electric field has begun to extend into the grids at the extraction voltage of −500 V, which means that the plasma emission surface becomes concave surface at this time.

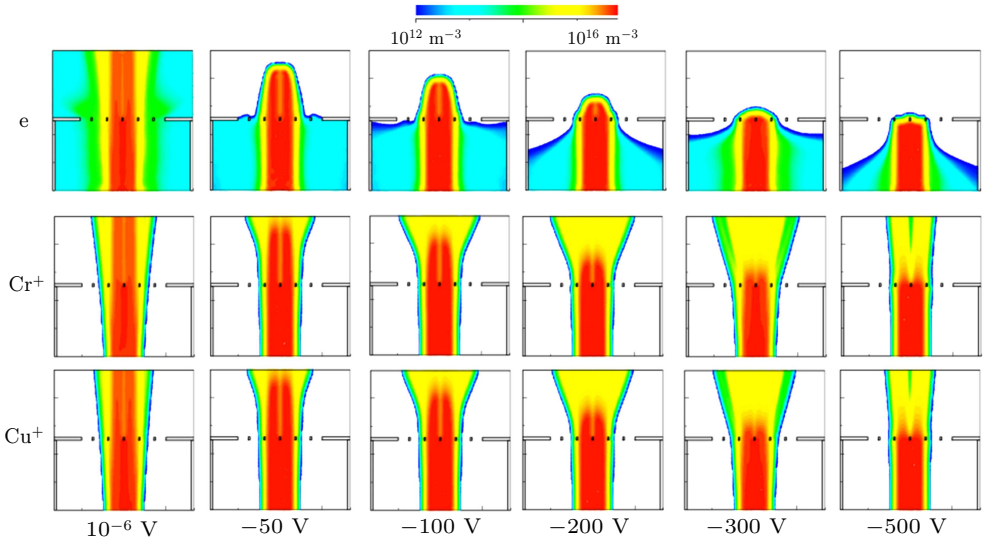


Fig. 3. Density distributions under different extraction voltages.

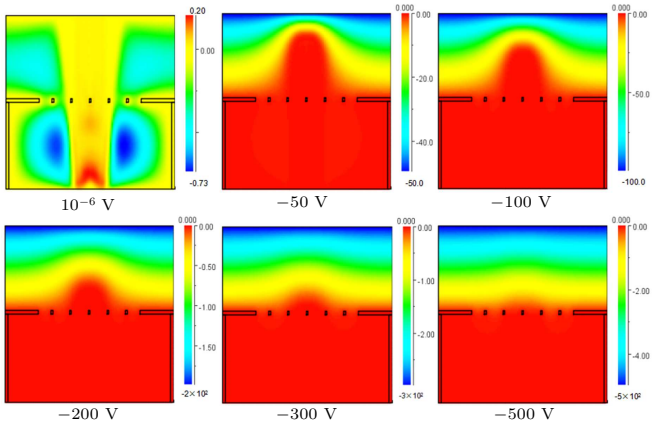


Fig. 4. Potential distributions under different extraction voltages.

The influence of different extraction voltages on the number density distribution of Cr$^+$ and Cu$^+$ at the extraction electrode are shown in Figs. 6 and 7, respectively. It can be found that the density distributions of Cr$^+$ ions and Cu$^+$ ions at the extraction electrode vary with the different extraction voltages. Under same extraction voltages, the density distributions of Cr$^+$ ions and Cu$^+$ ions at the extraction electrode are generally similar, and the distribution range of Cr$^+$ ions is slightly larger than that of Cu$^+$ ions, while the density of Cr$^+$ ions at the same position is slightly smaller than that of Cu$^+$ ions. This means that when Cr$^+$ and Cu$^+$ ions are extracted the movement behavior of different kinds of ions is not completely the same.

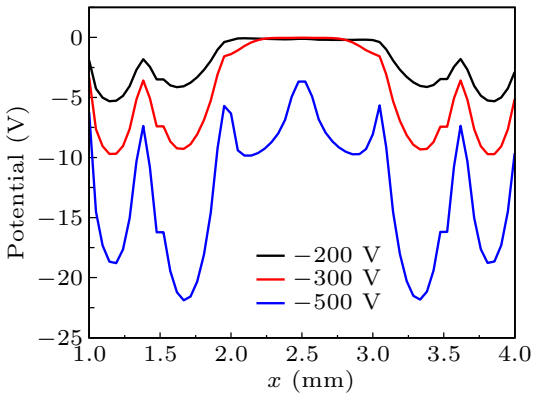


Fig. 5. Potential distributions at the grids under different extraction voltages.

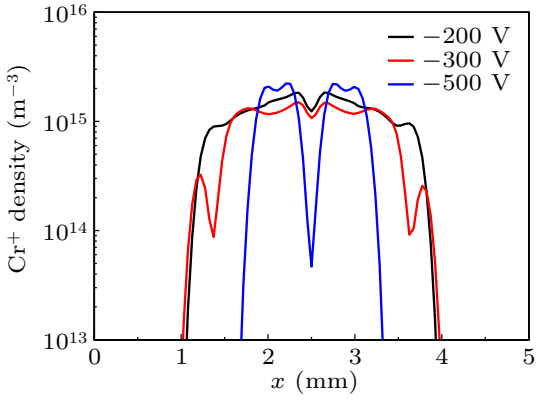


Fig. 6. Density distributions of Cr$^+$ ions under different extraction voltages.

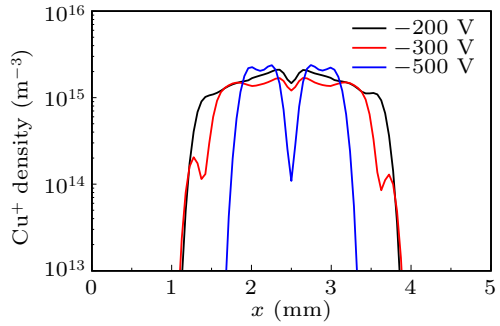


Fig. 7. Density distributions of Cu^+ ions under different extraction voltages.

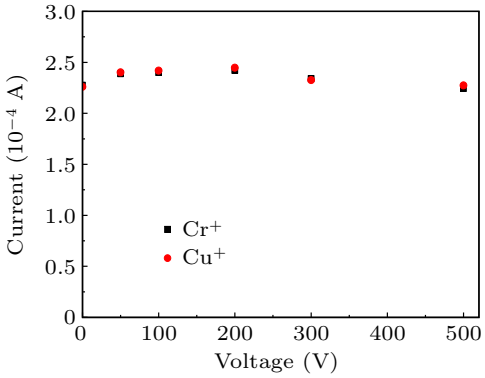


Fig. 8. Ion currents under different extraction voltages.

The 2D simulation cannot directly obtain the ion beam current, only the current density distribution can be calculated. Assuming that the simulation results within 1 mm perpendicular to the simulation area are the same, the ion beam current under different extraction voltages can be calculated. The results obtained by simulation are shown in Fig. 8. It can be seen that the currents of Cr^+ ions and Cu^+ ions are basically the same under different extraction voltages.

4. Discussion

In the simulations, the initial parameters of Cr^+ ions and Cu^+ ions are the same. The density distributions of the two ions are the same in the plasma chamber, while the density distributions of the two ions at the extraction electrode are different. This shows that after electrons and positive ions are separated, some factors lead to the different motion behaviors of Cr^+ ions and Cu^+ ions. In theory, ions are only affected by the induced electric field and the space charge field between ions at this time. These two kinds of electric fields have nothing to do with ion species, so it should be some characteristics of ions themselves that lead to different motion behaviors of different ions species under the same force.

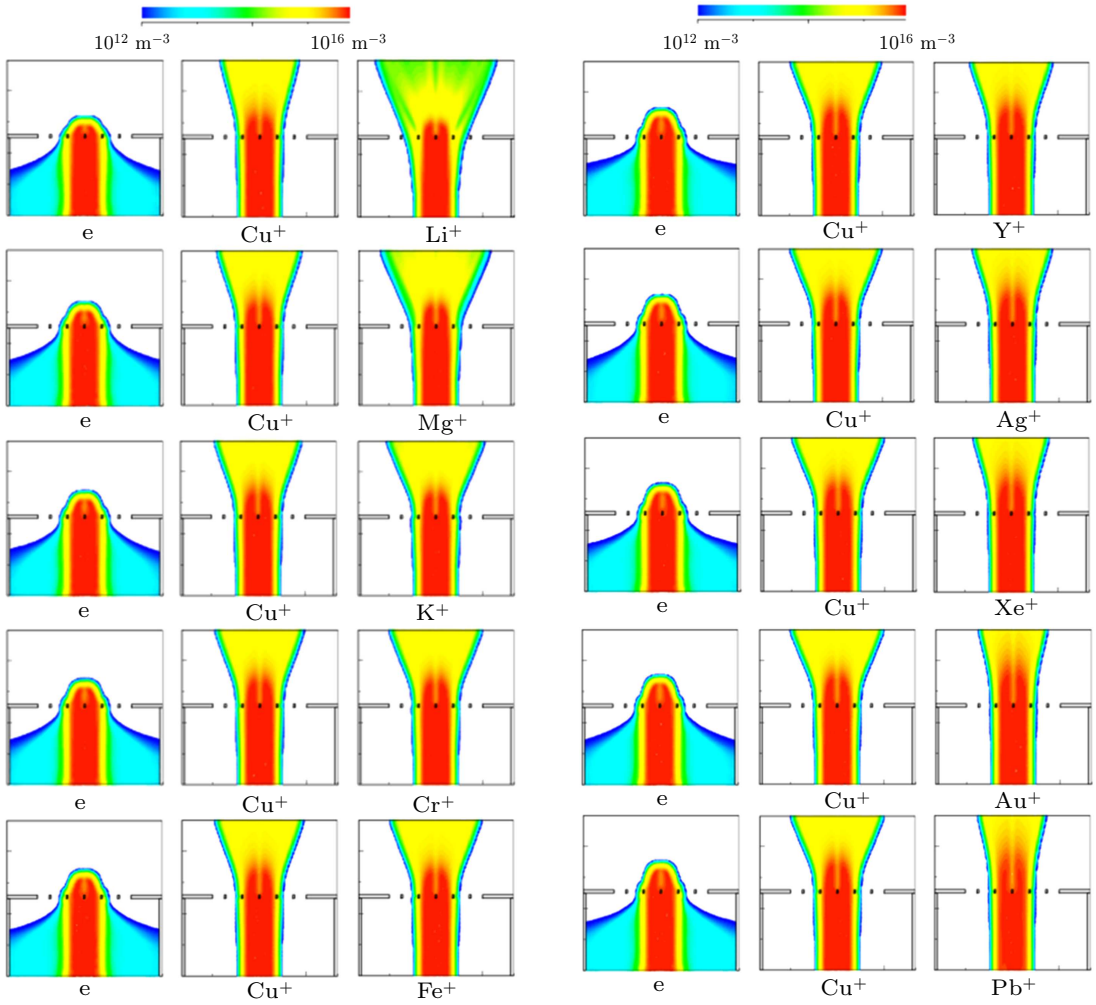


Fig. 9. Density distributions with different mixed ions.

In order to understanding the phenomenon, based on the same simulation model, only Cr^+ ions replaced with nine kinds of ions, such as Li^+, Mg^+, K^+, Fe^+, Y^+, Ag^+, Xe^+, Au^+, Pb^+, the particle number density distributions of different kinds of mixed ions at 3.0 μs are simulated respectively under the condition that the extraction voltage amplitude is 200 V. The reason we chose 200 V is that electrons and ions are separated outside the plasma chamber, which can effectively eliminate the influence of the extraction voltage extending into the plasma chamber on the ion motion behavior. The results are shown in Fig. 9. When Cu^+ ions are mixed with different kinds of ions, not only the density distributions of Cu^+ ions at the extraction electrode are different, but also the density distributions of different kinds of ions at the extraction electrode is different.

In order to analyze which ionic characteristics lead to this difference described above, we sorted the atomic radius of these nine ions and Cr^+ ions, and obtained the corresponding relationship with the density distribution region of ions at the extraction electrode which is the length of ion distribution at the extraction electrode indicating the ion diffusion degree. The results are shown in Fig. 10, it can be seen that the ion diffusion degree has no obvious correlation with the corresponding atomic radii of these ions.

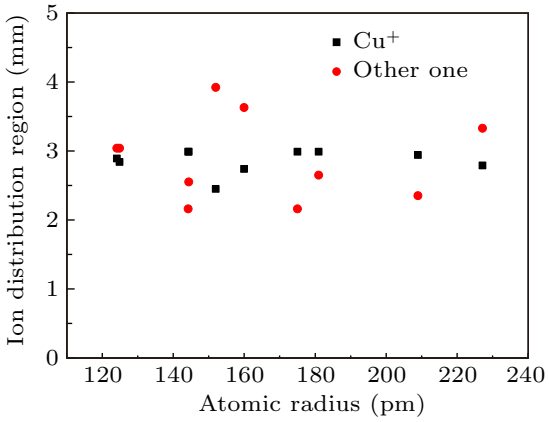


Fig. 10. Ion distribution region versus corresponding atomic radius.

Further sorting the atomic masses corresponding to these ten kinds of ions, we obtained the relationship between the density distribution region of ions at the extraction electrode and their corresponding atomic masses, as shown in Fig. 11. When the atomic mass of the ions mixed with Cu^+ ions is less than the atomic mass of Cu which is 63.5, the diffusion degree of these ions increases with the decrease of their corresponding atomic masses, while the diffusion degree of Cu^+ ions decreases. When the atomic mass of the ions mixed with Cu^+ ions is larger than that of Cu, the diffusion degree of these ions decreases with the increase of their atomic mass, but the diffusion degree of Cu^+ ions has no significant change. This demonstrates that atomic mass is the key factor affecting the diffusion distribution of different ions during the extraction of mixed ions. As the space charge force causing ion diffusion is only related to the charge distribution, in the simulation, there should be little difference between different kinds of ions in space charge force, which leads to the lighter ions being moved and diffused more easily by space charge force.

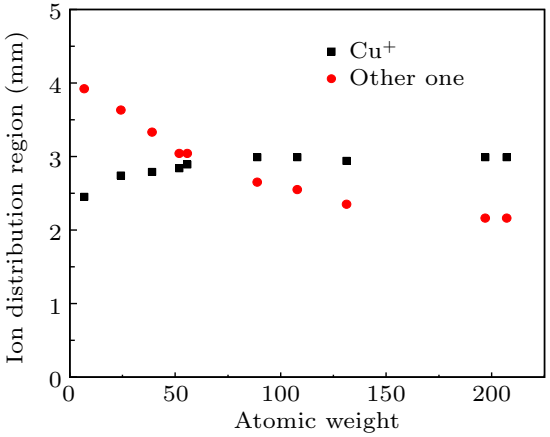


Fig. 11. Ion distribution region versus corresponding atomic mass.

Besides, the relationship between the maximum moving distance of electrons in the *Y* direction and their corresponding atomic masses are shown in Fig. 12. With the increase of the atomic masses corresponding to the extracted ions, the maximum moving distance of electrons in the *Y* direction increases at first and then rate of increase gradually slows down. The separation of electrons and ions not only affected by the amplitude of the extracted voltage, but also affected by the space charge force. The lighter ions are easier to diffuse, leading to a rapid decrease in density after separated from electrons. Therefore, the attraction of ion beams to electrons will decrease rapidly, thus making electrons unable to move in the *Y* direction. On the contrary, the heavier ion beam can attract electrons to move further. However, when the mass increases to a certain extent, the divergence degree of Cu^+ ion is basically unchanged, and the divergence degree of the other ion varies slowly with the increase of the corresponding atomic mass, so the increase of the distance of electron moving in *Y* direction also slows down obviously.

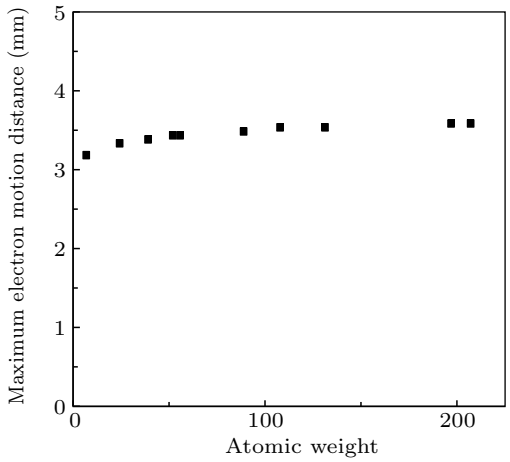


Fig. 12. Maximum moving distance of the electron versus corresponding atomic mass.

5. Conclusion

The distribution of Cr^+ ions and Cu^+ ions at the extraction electrode is generally similar when Cr^+ and Cu^+ ions are extracted under different extraction voltages, but the distribution range of Cr^+ ions is slightly larger and the density is slightly lower than that of Cu^+ ions. Furthermore, through the simulation of Cu^+ ions mixed with nine kinds of ions respectively, it is revealed that the atomic mass is the key factor leading to the different density distribution when different ions are mixed and extracted. The reason is that the lighter the mass of ions, the easier it is to move and diffuse by space charge force. This provides a support for further deepening the ion extraction characteristics.

Acknowledgements

Project supported by the Presidential Foundation of China Academy of Engineering Physics (Grant No. YZJJZQ2022016) and the National Natural Science Foundation of China (Grant No. 52207177).

References

[1] Brown I G and Oks E M 2005 *IEEE Transs. Plasma Sci.* **33** 1931
[2] Nikolaev A G, Oks E M, Savkin K P, Yushkov G Yu, Frolova V P and Barengolts S A 2014 *J. Appl. Phys.* **116** 213303
[3] Li J, Yang F X, Fan Z L, Du W D and Xu A 2022 *IEEE Trans. Plasma Sci.* **50** 1097
[4] Kosonen S T, Kalvas T, Tarvainen O and Toivanen V 2022 *J. Phys.: Conf. Ser.* **2244** 012079
[5] Abdelrahman M M 2012 *Ain Shams Engineering Journal* **3** 71
[6] Li H L and Sun A B 2021 *Comput. Phys. Commun.* **259** 107629
[7] Abdelrahman M M, Basal N I and Zakhary S G 2012 *Chin. Phys. C* **36** 344
[8] Xu A, Gan P P, Shi Y J and Chen L 2024 *Chin. Phys. B* **33** 045203
[9] Shmelev D L, Barengolts S A, Uimanov I V, Tsventoukh M M and Savkin K P 2015 *J. Phys.: Confer. Ser.* **652** 012041
[10] Keller R 1990 *Nuclear Instruments and Methods in Physics Research A: Accelerators, Detectors, Associated Equipment* **298** 247
[11] Chen J, Fu T Z, Guo H, Li H P, Jiang D J and Zhou M S 2019 *Plasma Sci. Technol.* **21** 045402
[12] Benilov M S 2009 *Plasma Sources Sci. Technol.* **18** 014005
[13] Masamune S and Yukimura K 2006 *IEEE Trans. Plasma Sci.* **34** 1195
[14] Mandl S, Gunzel R and Moller W 1998 *J. Phys. D: Appl. Phys.* **31** 1109
[15] Baalrud S D, Scheiner B, Yee B T, Hopkins M M and Barnat E 2020 *Plasma Sources Science and Technology* **29** 053001
[16] Garner A L, Darr A M and Harsha N R S 2022 *IEEE Trans. Plasma Sci.* **50** 2528
[17] Huang H and Liu Y J 2019 *IEEE Trans. Plasma Sci.* **47** 3631
[18] Lafleur T and Aanesland A 2014 *Phys. Plasmas* **21** 123506
[19] Lu Q M, Guo J, Dou X K and Wang S 2004 *Chin. J. Comput. Phys.* **21** 137
[20] Xu A, Shi Y J, Zhong W, Jin D Z and Chen L 2022 *IEEE Trans. Plasma Sci.* **50** 769
[21] Xu A, Yang L, Zhong W, Liu Y L, Shang S H and Jin D Z 2018 *High Voltage Engineering* **44** 1922
[22] Xu A, Jin D Z, Wang Y J and Tan X H 2020 *IEEE Trans. Plasma Sci.* **48** 888
[23] Xu A, Wang Y J, Du J S, Jin D Z and Chen L 2021 *High Voltage Engineering* **47** 4134
[24] Xu A, Jin D Z, Wang Y J, Chen L and Tan X H 2020 *High Voltage Engineering* **46** 715